

## RESEARCH ARTICLE

# Novel spreading codes for multicarrier code division multiple access based cognitive radio networks with sidelobe suppression

Morteza Rajabzadeh\* and Hossein Khoshbin

Electrical Engineering Department, Ferdowsi University of Mashhad, Mashhad, Iran

## ABSTRACT

The deployment of multicarrier code division multiple access as the transmission scheme of the spectrum overlay based cognitive radio (CR) networks faces two challenging issues: (i) the need for spreading codes with arbitrary length and (ii) the interfering effect of the leaked power (due to spectral sidelobes) to the adjacent spectral band used by the primary system. To meet these challenges, we propose two novel complex spreading code sets. For this purpose, a cost function is defined as the ratio of the power leaked to the adjacent primary band to the power transmitted to the band allowed for CR operation. The cost function is shown to be convertible to a trace ratio problem. The two complex spreading code sets are determined by deploying two different standard solutions. The first is the conventional but approximate solution based on generalized eigenvalue decomposition (GEVD) method, and the other is an iterative algorithm that converges to the optimal solution and hence outperforms the GEVD based solution. Simulation results show that by a slight decrease in number of users, the code set yielded by iterative algorithm suppresses the leaked power to almost zero. The applicability of the proposed code sets in different scenarios is discussed. Copyright © 2012 John Wiley & Sons, Ltd.

## KEYWORDS

cognitive radio; MC-CDMA; sidelobe suppression; spreading code design

### \*Correspondence

Morteza Rajabzadeh, Electrical Engineering Department, Ferdowsi University of Mashhad, Mashhad, Iran.

E-mail: morteza.rajabzade@gmail.com

## 1. INTRODUCTION

Recently, opportunistic usage of licensed frequency bands has been proposed as a solution to the spectrum scarcity problem by deploying cognitive radio (CR) systems. In the basic definition [1], CRs have a broad range of sensing, learning and acting capabilities converting them to smart autonomous radios. Current requirements of wireless transmission and implementation challenges have highlighted some of these capabilities. Among them are the efficient secondary spectrum access and the shift from autonomous CR functioning, which is more suitable for *ad hoc* networking utilization, to structured networking architectures [2]. Working in overlay mode [3,4], the secondary user (SU) would be able to opportunistically deploy the unused parts of a licensed band. In order to use these spectrum holes while minimizing the interference on the adjacent primary system band, the SU must shape its signal spectrum. Multicarrier (MC) techniques, especially multicarrier code division multiple access (MC-CDMA) and orthogonal frequency division multiplexing (OFDM)

are considered as candidate transmission schemes for such applications [3–8].

In this paper, the spreading code design for downlink of the MC-CDMA based CR network has been addressed. When MC-CDMA system works in the overlay mode [3,4], it must null the subcarriers that are inside the band used by the primary transmission. Two challenges arise here. The first challenge is the need for the set of spreading codes with any arbitrary length because the number of remaining data subcarriers would be any integer value. The most widely proposed solution is the utilization of complex carrier interferometry (CI) codes [3,9–11]. The second challenge is the power leakage to the adjacent frequency bands licensed to primary system that is due to the unwanted large spectral sidelobes of the active subcarriers. This is an intrinsic drawback of Fourier based MC transmission [8,12]. To mitigate the spectral sidelobes problem, a wide variety of approaches have been proposed for OFDM technique in the literature. The simplest method, the insertion of guard band, sacrifices bandwidth because the spectral fall-off of the Fourier based MC

transmission is small [12]. Pulse shaping and windowing approaches extend the required cyclic prefix (CP) length [13]. In an important class of sidelobe suppression methods known as active interference cancelation (AIC) [14,15] and cancelation carrier (CC) [16], the data transmitted on the tones adjacent to the band occupied by the primary users (PUs) are designed to suppress the interfering sidelobes. Although these methods provide a good level of protection to the primary system, a remarkable part of each OFDM symbol power must be allocated to the AIC (CC) tones. The addition of designed redundancy to each OFDM symbol (adaptive symbol transition (AST) method [17]) is another approach that lengthens the OFDM symbol and requires more cyclic prefix length. The data tones can be precoded by orthogonal precoding vectors suggested for discrete Fourier transform based [18] and analog [12,19,20] OFDM implementations. Subcarrier weighting [21] and additive methods [22] are two other methods with poor sidelobe suppression performance that also degrade the bit error rate performance of the system. Good sidelobe suppression of about 80 dB is obtained by a variant of AIC, called extended AIC, but at the expense of considerable bit error rate (BER) performance loss [14]. With the combination of CC and modulated filter banks, arbitrary sidelobe suppression level is acquired, but this needs a wide transition band that sacrifices the system throughput [23].

All the above-mentioned techniques require extra redundancy or extra processing to be added to the OFDM symbols. Although these methods are also applicable to MC-CDMA, we have proposed to deploy an inherent attribute of MC-CDMA, the use of spreading codes, for the purpose of sidelobe suppression without the need for any extra redundancy or processing. To the best of our knowledge, this idea has not been reported in the literature yet. In conventional MC-CDMA transmission, the data symbols of each of the users are spread on all the available subcarriers spanning the spectral band allocated to the MC-CDMA system. We have considered the situation where the PUs deploy some parts of the band allocated to the secondary MC-CDMA system. Our aim is to prevent the leakage of the available power to the primary system band. So, the ratio of the power leaked to the PUs' band to the power in the SU band is considered as the objective function that should be minimized. We have shown that this nonlinear cost function can be converted to a standard problem known as trace ratio (TR) problem [24]. The proposed complex spreading code sets are determined by solving the achieved TR problem by two readily available approaches. The first approach is an approximate solution deploying generalized eigenvalue decomposition (GEVD) method. The second approach is an iterative algorithm. It is proved in the literature that the iterative algorithm converges to the optimal solution.

Simulation results show that the two proposed approaches provide outstanding sidelobe suppression level. The iterative method outperforms the GEVD based method because of its optimality. However, the computational complexity

of the iterative method is slightly more than the GEVD based method. In both methods, the sidelobe suppression performance is a function of system throughput (in terms of number of active users). It is shown that by a slight decrease in the number of active users ( $K$ ) with respect to (w.r.t.) fully loaded case, the iterative approach is able to suppress the spectral sidelobes to almost zero, without the need for considerable guard band. The amount of decrement in  $K$  is a function of the spectral position and characteristics of the primary system. Unlike the AST, subcarrier weighting and the variants of AIC and CC methods, which require recalculating the parameter used for sidelobe suppression at *each* transmitted OFDM symbol, there is no need to recalculate the spreading codes for each transmitted MC-CDMA symbol. The codes are valid until the next spectral repositioning of the PUs. In addition, the problem of the codes length to be arbitrary is resolved by the proposed spreading codes. These complex codes have the crucial orthogonality condition needed for the MC-CDMA working in multiuser mode.

The paper is organized as follows. After the introduction, downlink MC-CDMA system model and its power spectrum are introduced in Section 2. The leaked power avoidance problem is formulated in Section 3 as a TR optimization problem for which two solutions are proposed in Section 4 designing spreading code sets. Performance evaluations and comparisons are considered in Section 5 by computer simulations, and the paper is concluded in Section 6.

## 2. SYSTEM MODEL

The downlink transmission of a wideband CR system with  $K$  active users is considered, where MC-CDMA technique with  $L$  subcarriers is adopted as both the physical layer and the multiple access schemes. The CR system is allowed to deploy parts of a fixed spectrum that are not used by the primary system. We assume that the spectral position of the primary transmission is known at the base station (BS) of the CR system. The deactivation of the subcarriers inside this band is not enough to avoid interference on the band used by the PUs because of the large spectral sidelobes of the adjacent data-bearing subcarriers. Therefore, the secondary BS designs the spreading codes of the users such that the leaked power to the band of the PUs is minimized.

In the BS of the secondary network, the modulated data symbol of the  $k$ th user at time instant  $n$ ,  $d_k(n)$ , is spread by a distinct spreading code vector,  $\mathbf{c}_k$ , with the size  $L \times 1$ . The spread data vectors of different users are added to form the frequency domain data vector, that is,

$$\mathbf{x}(n) = \sum_{k=1}^K \mathbf{c}_k d_k(n) = \mathbf{C}\mathbf{d}(n) \quad (1)$$

where  $\mathbf{d}(n) = [d_1(n), d_2(n), \dots, d_K(n)]^T$  is the  $K \times 1$  vector containing the data symbols of different users and  $\mathbf{C} = [\mathbf{c}_1, \mathbf{c}_2, \dots, \mathbf{c}_K]$  is the  $L \times K$  spreading code matrix

containing the codes of all active users. Also, we have  $\mathbf{x}(n) = [x_0(n), x_1(n), \dots, x_{L-1}(n)]^T$ . Without loss of generality, it is assumed that the spreading codes are orthogonal with unit power, that is,  $\mathbf{C}^H \mathbf{C} = \mathbf{I}_K$ , where  $\mathbf{I}_K$  is the  $K \times K$  identity matrix. In this way, the average transmitted power of each user at the frequency domain is constrained to one.

The frequency domain data is converted into the time domain by inverse discrete Fourier transform. After adding the cyclic prefix, the time domain samples are obtained as follows:

$$s_m(n) = \frac{1}{\sqrt{L}} \sum_{l=0}^{L-1} x_l(n) e^{j2\pi(m-\nu)\frac{l}{L}},$$

$$m = 0, 1, \dots, M-1 \quad (2)$$

where  $\nu$  is the CP length and  $M = L + \nu$ . Also,  $x_l(n)$  is the frequency domain data transmitted on the  $l$ th subcarrier. The  $M \times 1$  time domain data vector,  $\mathbf{s}(n) = [s_0(n), s_1(n), \dots, s_{M-1}(n)]^T$ , formed by the accumulation of time domain samples, can be represented in the vector form as follows:

$$\mathbf{s}(n) = \mathbf{F}^H \mathbf{D} \mathbf{x}(n) \quad (3)$$

where  $\mathbf{F}_{L \times M}$  is a Fourier matrix with the  $(l, m)$ th entry  $[F]_{l,m} = (1/\sqrt{L})e^{-j2\pi lm/L}$ , and  $\mathbf{D} = \text{diag}(1, e^{-j2\pi\nu/L}, \dots, e^{-j2\pi\nu(L-1)/L})$  is an  $L \times L$  diagonal matrix that models the CP addition. The  $N_s$ -upsampled in-band spectrum of the MC-CDMA transmitter is characterized by the following [15]:

$$y_i^{(n)} = \sum_{m=0}^{M-1} s_m(n) e^{-j2\pi m \frac{i}{N_s L}}, \quad i = 0, 1, \dots, N_s L - 1 \quad (4)$$

The  $N_s$ -upsampled spectral samples can be accumulated in an  $N_s L \times 1$  vector as follows:

$$\mathbf{y}^{(n)} = \mathbf{E} \mathbf{s}(n) = \mathbf{E} \mathbf{F}^H \mathbf{D} \mathbf{C} \mathbf{d}(n) \quad (5)$$

where  $\mathbf{E}$  is the  $N_s L \times M$  upsampled Fourier matrix with the  $(i, m)$ th entry  $[\mathbf{E}]_{i,m} = e^{-j2\pi m \frac{i}{N_s L}}$ . On the basis of the described frequency spectrum of the secondary MC-CDMA transmitter, the interference of the secondary transmission on the primary band is modeled in the next section, and the optimization problem to design the spreading codes is developed.

At the receiver of the  $m$ th user, after CP removal and FFT processing, the received  $L \times 1$  vector can be written as follows:

$$\mathbf{r} = \mathbf{H}_m \mathbf{c}_m d_m + \mathbf{H}_m \sum_{\substack{k=1 \\ k \neq m}}^K \mathbf{c}_k d_k + \boldsymbol{\xi}_m \quad (6)$$

in which  $\mathbf{H}_m$  is an  $L \times L$  diagonal matrix whose  $(l, l)$ th entry is equal to the  $l$ th discrete Fourier transform

coefficient of the channel impulse response between the secondary BS and the  $m$ th user. Also,  $\boldsymbol{\xi}_m$  is the complex additive white Gaussian noise vector with zero mean and covariance matrix  $\mathbf{R}_{\boldsymbol{\xi}} = \sigma_{\boldsymbol{\xi}}^2 \mathbf{I}_L$ . For the detection, we simply use the inverse of the channel matrix to undo the channel effect. Hence, if the deployed spreading codes are orthogonal, multiuser interference can be fully mitigated. After despreading, we have

$$\hat{d}_m = \mathbf{c}_m^H \mathbf{H}_m^{-1} \mathbf{r} = d_m + \mathbf{c}_m^H \left( \sum_{\substack{k=1 \\ k \neq m}}^K \mathbf{c}_k d_k + \mathbf{H}_m^{-1} \boldsymbol{\xi}_m \right)$$

$$= d_m + \mathbf{c}_m^H \mathbf{H}_m^{-1} \boldsymbol{\xi}_m \quad (7)$$

### 3. PROBLEM FORMULATION

Assume that the CR system detects the signal of a PU spanning over  $N_{\text{PU}}$  subcarriers denoted by the set  $I_{\text{PU}} = \{\sigma_1, \sigma_1 + 1, \dots, \sigma_2\}$ . Obviously,  $N_{\text{PU}} = \sigma_2 - \sigma_1 + 1$ . On each side of the primary transmission,  $\gamma$  subcarriers are considered as guard band. The secondary BS should minimize the leaked power to the part of its band covering the subcarriers indexed as  $I_{\text{PU-GB}} = \{\sigma_1 - \gamma, \dots, \sigma_1, \sigma_1 + 1, \dots, \sigma_2, \dots, \sigma_2 + \gamma\}$ , which we call PU-GB. Because there are  $N_{\text{GB}} = 2\gamma$  guard band subcarriers, the number of the remaining subcarriers used for data transmission is  $N_{\text{D}} = L - (N_{\text{PU}} + N_{\text{GB}})$ . Clearly, the number of active users for the system to be fully loaded is  $K^{\text{FL}} = N_{\text{D}}$ .

In (5), the  $N_s$ -upsampled spectrum of the MC-CDMA is introduced. It is evident that it is a function of the transmitted data symbols of the active users, the spreading code set and the size of CP. In a secondary scenario, when some part of the available band is occupied by the PUs, the spectral samples located at the PU band must be minimized. At the same time, the available power must be allocated to the vacant portion of the band. On the basis of this philosophy, we define the ratio between the leaked power to primary and guard band ( $P_{\text{P}}$ ) to the power in the remaining data-bearing subcarriers used for secondary transmission ( $P_{\text{S}}$ ) as the cost function to be minimized by designing the spreading code sets of the active users. Thus, the objective function for the problem at hand is

$$\min_{\mathbf{C}} \frac{P_{\text{P}}}{P_{\text{S}}}, \quad \text{subject to } \mathbf{C}^H \mathbf{C} = \mathbf{I}_K \quad (8)$$

The applied constraint makes the spreading codes orthogonal. Moreover, it limits the average transmitted power of each user at the frequency domain to one (as we have in relation (1)).

In order to determine the leaked power, consider the upsampled frequency spectrum in (4) and (5). The subset of indices of the upsampled spectrum within the PU and guard band is  $\Gamma_{\text{PU}}^{\text{GB}} = \{N_s(\sigma_1 - \gamma), N_s(\sigma_1 - \gamma) + 1, \dots, N_s(\sigma_2 + \gamma) - 1, N_s(\sigma_2 + \gamma)\}$  that consists of  $N_{\text{PU,GB}}^{\text{up}} = N_s(\sigma_2 - \sigma_1) + N_s(2\gamma) + 1$  samples. A new

matrix,  $\mathbf{E}_P$ , is formed that is a submatrix of  $\mathbf{E}$  containing only those rows of  $\mathbf{E}$  whose indices are in the set  $\Gamma_{PU}^{GB}$ , arranged in their natural order. Clearly, the size of  $\mathbf{E}_P$  is  $N_{PU,GB}^{up} \times M$ . Therefore, the upsampled spectrum of the secondary transmission at the PU and guard bands can be determined by deploying  $\mathbf{E}_P$  instead of  $\mathbf{E}$  in (5). Because the data vector  $\mathbf{d}(n)$  is composed of random processes, the samples  $y_i^{(n)}$  are also random processes. Hence, the average leaked power to the PU-GB can be defined as

$$P_P = E \left\{ \left\| \mathbf{y}_P^{(n)} \right\|_2^2 \right\} = E \left\{ \left\| \mathbf{E}_P \mathbf{F}^H \mathbf{D} \mathbf{C} \mathbf{d}(n) \right\|_2^2 \right\} \quad (9)$$

in which  $\|\cdot\|_2$  denotes 2-norm,  $E\{\cdot\}$  is the expectation operator and  $\mathbf{y}_P^{(n)}$  is the upsampled spectrum of the secondary transmission at the PU and guard bands. In other words,  $\mathbf{y}_P^{(n)}$  is a subset of samples of  $\mathbf{y}^{(n)}$  whose indices are denoted by  $\Gamma_{PU}^{GB}$ . The leaked power,  $P_P$ , can be rewritten as

$$P_P = E \left\{ \mathbf{d}^H(n) \mathbf{C}^H \mathbf{D}^H \mathbf{F} \mathbf{E}_P^H \mathbf{E}_P \mathbf{F}^H \mathbf{D} \mathbf{C} \mathbf{d}(n) \right\} \quad (10)$$

The allocated power to the secondary transmission on the data-bearing subcarriers,  $P_S$ , can be expressed in a similar manner. The subset of indices of the upsampled spectrum within the allowed data-band for the SUs is  $\Gamma_{SU} = \{i \mid 0 \leq i \leq N_s L - 1, i \notin \Gamma_{PU}^{GB}\}$ . Clearly,  $\Gamma_{SU} \cup \Gamma_{PU}^{GB} = \{0, 1, \dots, N_s L - 1\}$ . The average power transmitted in the data-band is as follows:

$$\begin{aligned} P_S &= E \left\{ \left\| \mathbf{y}_S^{(n)} \right\|_2^2 \right\} = E \left\{ \left\| \mathbf{E}_S \mathbf{F}^H \mathbf{D} \mathbf{C} \mathbf{d}(n) \right\|_2^2 \right\} \\ &= E \left\{ \mathbf{d}^H(n) \mathbf{C}^H \mathbf{D}^H \mathbf{F} \mathbf{E}_S^H \mathbf{E}_S \mathbf{F}^H \mathbf{D} \mathbf{C} \mathbf{d}(n) \right\} \end{aligned} \quad (11)$$

where  $\mathbf{y}_S^{(n)}$  is a subset of samples of  $\mathbf{y}^{(n)}$  whose indices are denoted by  $\Gamma_{SU}$  and  $\mathbf{E}_S$  is formed by selecting the rows of  $\mathbf{E}$  indexed by  $\Gamma_{SU}$ . Considering the relations found above for  $P_P$  and  $P_S$ , the optimization problem given in (8) is hard to solve. So we try to convert it to a tractable problem. The relation (10) is in the form  $P_P = E \left\{ \mathbf{a}^H(n) \mathbf{a}(n) \right\}$  where  $\mathbf{a}(n) = \mathbf{E}_P \mathbf{F}^H \mathbf{D} \mathbf{C} \mathbf{d}(n)$  is an  $N_{PU,GB}^{up} \times 1$  vector. It is easy to investigate that  $\mathbf{a}^H(n) \mathbf{a}(n) = \text{Tr}[\mathbf{a}(n) \mathbf{a}^H(n)]$  where  $\text{Tr}[\cdot]$  is the linear trace operator [25]. So,  $P_P$  in (10) can be rephrased as

$$\begin{aligned} P_P &= E \left\{ \text{Tr} \left[ \mathbf{a}(n) \mathbf{a}^H(n) \right] \right\} \\ &= E \left\{ \text{Tr} \left[ \mathbf{E}_P \mathbf{F}^H \mathbf{D} \mathbf{C} \mathbf{d}(n) \mathbf{d}^H(n) \mathbf{C}^H \mathbf{D}^H \mathbf{F} \mathbf{E}_P^H \right] \right\} \end{aligned} \quad (12)$$

Both the expectation and trace operators are linear. Thus, they can be swapped, and (12) becomes

$$\begin{aligned} P_P &= \text{Tr} \left[ E \left\{ \mathbf{E}_P \mathbf{F}^H \mathbf{D} \mathbf{C} \mathbf{d}(n) \mathbf{d}^H(n) \mathbf{C}^H \mathbf{D}^H \mathbf{F} \mathbf{E}_P^H \right\} \right] \\ &= \text{Tr} \left[ \mathbf{E}_P \mathbf{F}^H \mathbf{D} \mathbf{C} E \left\{ \mathbf{d}(n) \mathbf{d}^H(n) \right\} \mathbf{C}^H \mathbf{D}^H \mathbf{F} \mathbf{E}_P^H \right] \end{aligned} \quad (13)$$

The elements of the data vector  $\mathbf{d}(n)$  are the modulated data symbols of different users. If we assume that the data symbols of different users are independent and identically distributed (i.i.d.) such that  $E \left\{ \mathbf{d}(n) \mathbf{d}^H(n) \right\} = \mathbf{I}_K$ , we have

$$P_P = \text{Tr} \left[ \mathbf{E}_P \mathbf{F}^H \mathbf{D} \mathbf{C} \mathbf{C}^H \mathbf{D}^H \mathbf{F} \mathbf{E}_P^H \right] \quad (14)$$

Applying the fact that  $\text{Tr}[\mathbf{A}\mathbf{B}] = \text{Tr}[\mathbf{B}\mathbf{A}]$  to (14), the leaked power to the PU-GB is converted to

$$P_P = \text{Tr} \left[ \mathbf{C}^H \mathbf{P} \mathbf{C} \right] \quad (15)$$

where

$$\mathbf{P} = \mathbf{D}^H \mathbf{F} \mathbf{E}_P^H \mathbf{E}_P \mathbf{F}^H \mathbf{D} \quad (16)$$

is a symmetric and positive semi-definite  $L \times L$  matrix.

By applying the above procedure to relation (11), it is easy to show that  $P_S$  can be expressed as follows:

$$P_S = \text{Tr} \left[ \mathbf{C}^H \mathbf{S} \mathbf{C} \right] \quad (17)$$

where

$$\mathbf{S} = \mathbf{D}^H \mathbf{F} \mathbf{E}_S^H \mathbf{E}_S \mathbf{F}^H \mathbf{D} \quad (18)$$

is a symmetric and positive semi-definite  $L \times L$  matrix. Substituting  $P_P$  and  $P_S$  in (8), our optimization problem becomes as follows:

$$\min_{\mathbf{C}} \frac{\text{Tr}[\mathbf{C}^H \mathbf{P} \mathbf{C}]}{\text{Tr}[\mathbf{C}^H \mathbf{S} \mathbf{C}]}, \quad \text{subject to } \mathbf{C}^H \mathbf{C} = \mathbf{I}_K \quad (19)$$

The optimization of the above form is known as the TR problem [24]. In the literature, two different solutions are proposed to solve this problem. By deploying these solutions, two different orthogonal complex spreading code sets are proposed in the next section. Moreover, some discussions of the feasibility of these code sets are given.

## 4. SPREADING CODE DESIGN

### 4.1. NC-GEVD spreading code set

The TR problem in (19) does not have a closed-form global optimum solution. Conventionally, this problem is converted to the following ratio trace problem [24]:

$$\mathbf{C}^{\text{NC-GEVD}} = \arg \min \text{Tr} \left[ (\mathbf{C}^H \mathbf{S} \mathbf{C})^{-1} (\mathbf{C}^H \mathbf{P} \mathbf{C}) \right] \quad (20)$$

which can be efficiently solved by GEVD method. Specifically, the solution is the invariant subspace of eigenvectors corresponding to  $K$  smallest eigenvalues of  $\mathbf{S}^{-1} \mathbf{P}$ . We call the non-contiguous MC-CDMA secondary system whose code is determined by the above approach as NC-GEVD.

## 4.2. NC-ITR spreading code set

The solution in (20) is an approximate solution of the main problem. In [26], an iterative algorithm is proposed to solve (19), which is called iterative trace ratio (ITR). Here, we first give a summary of the underlying idea of the algorithm and then describe the algorithm itself. It is not difficult to see that there is a minimum  $\lambda^*$  that is reached for a certain (non-unique) orthogonal matrix denoted by  $\mathbf{U}$ . For any orthogonal  $\mathbf{V}$ , we have  $\text{Tr}[\mathbf{V}^H \mathbf{P} \mathbf{V}] - \lambda^* \text{Tr}[\mathbf{V}^H \mathbf{S} \mathbf{V}] \geq 0$ , meaning that  $\text{Tr}[\mathbf{V}^H (\mathbf{P} - \lambda^* \mathbf{S}) \mathbf{V}] \geq 0$  and also  $\text{Tr}[\mathbf{U}^H (\mathbf{P} - \lambda^* \mathbf{S}) \mathbf{U}] = 0$ . Therefore, the necessary condition for the pair  $\lambda^*$  and  $\mathbf{U}$  to be optimal is given as

$$\min_{\mathbf{V}^H \mathbf{V} = \mathbf{I}_K} \text{Tr}[\mathbf{V}^H (\mathbf{P} - \lambda^* \mathbf{S}) \mathbf{V}] = \text{Tr}[\mathbf{U}^H (\mathbf{P} - \lambda^* \mathbf{S}) \mathbf{U}] = 0 \quad (21)$$

It is known that the minimum of trace of  $(\mathbf{P} - \lambda^* \mathbf{S})$  is simply the sum of the  $K$  smallest eigenvalues of  $(\mathbf{P} - \lambda^* \mathbf{S})$ , and  $\mathbf{U}$  is the set of corresponding eigenvectors. So, if  $\lambda^*$  minimizes the TR in (19), then the sum of  $K$  smallest eigenvalues of  $(\mathbf{P} - \lambda^* \mathbf{S})$  equals zero and the corresponding eigenvectors form the desired optimal solution of (19). For positive semi-definite  $\mathbf{S}$  and  $\mathbf{P}$ , it has been shown that [24,27] if  $\text{rank}[\mathbf{S}]$  is larger than  $L - K$  (or equivalently, if  $K$  is larger than the null space dimension of  $\mathbf{S}$ ,  $K > |\text{Null}(\mathbf{S})|$ ), then the following trace difference function

$$f(\lambda) = \min_{\mathbf{C}^H \mathbf{C} = \mathbf{I}_K} \text{Tr}[\mathbf{C}^H (\mathbf{P} - \lambda \mathbf{S}) \mathbf{C}] \quad (22)$$

is a non-increasing function and has a unique zero  $\lambda^*$ , which amounts to the global minimum of the TR in (19). Note that for fixed  $\lambda$ , the minimum value in (22) is achieved by deploying the orthonormal basis of eigenvectors associated with the  $K$  smallest eigenvalues of  $\mathbf{P} - \lambda \mathbf{S}$  denoted by  $\mathbf{C}(\lambda)$ . In summary, the TR optimization problem in (19) is equivalent to finding the unique root of  $f(\lambda)$  (i.e.,  $\lambda^*$ ) in (22), which can be found by using the iterative Newton method. For this purpose, the derivative of  $f(\lambda)$  is needed, which according to [24] is given as

$$f'(\lambda) = -\text{Tr}[\mathbf{C}(\lambda)^H \mathbf{S} \mathbf{C}(\lambda)] \quad (23)$$

Hence, the Newton method takes the form

$$\lambda^{\text{new}} = \lambda - \frac{\text{Tr}[\mathbf{C}(\lambda)^H (\mathbf{P} - \lambda \mathbf{S}) \mathbf{C}(\lambda)]}{-\text{Tr}[\mathbf{C}(\lambda)^H \mathbf{S} \mathbf{C}(\lambda)]} = \frac{\text{Tr}[\mathbf{C}(\lambda)^H \mathbf{P} \mathbf{C}(\lambda)]}{\text{Tr}[\mathbf{C}(\lambda)^H \mathbf{S} \mathbf{C}(\lambda)]} \quad (24)$$

The ITR procedure to find the spreading code sets that minimize the TR problem in (19) is stated in Algorithm 1. We denote the non-contiguous MC-CDMA scheme deploying this set of spreading codes as NC-ITR.

When  $K \leq |\text{Null}(\mathbf{S})|$ , a solution may be found by the ITR that satisfies  $\text{Tr}[\mathbf{C}^H \mathbf{S} \mathbf{C}] = 0$ , which draws the TR value to infinity. To avoid this, the null space of  $\mathbf{S}$  can be discarded from the solution space by principal component

---

### Algorithm 1 Iterative procedure to solve TR problem

---

**Input:** Two positive semi-definite matrices  $\mathbf{P}$  and  $\mathbf{S}$

**Output:** Trace ratio value  $\lambda^*$  and the optimal spreading code matrix  $\mathbf{C}^{\text{NC-ITR}}$

**Procedure:**

- (1) Initialize  $\mathbf{C}(\lambda^0)$  as an arbitrary column-wise orthogonal matrix;
- (2) For  $t = 1, 2, \dots, T^{\text{max}}$ , do
  - (a) Compute the TR value  $\lambda^t$  from  $\mathbf{C}(\lambda^{t-1})$ :

$$\lambda^t = \frac{\text{Tr}[\mathbf{C}(\lambda^{t-1})^H \mathbf{P} \mathbf{C}(\lambda^{t-1})]}{\text{Tr}[\mathbf{C}(\lambda^{t-1})^H \mathbf{S} \mathbf{C}(\lambda^{t-1})]}$$

- (b) Construct the trace difference problem as

$$\mathbf{C}(\lambda^t) = \arg \min_{\mathbf{C}^H \mathbf{C} = \mathbf{I}_K} \text{Tr}[\mathbf{C}^H (\mathbf{P} - \lambda^t \mathbf{S}) \mathbf{C}]$$

- (c) Solve the trace difference problem using eigenvalue decomposition method

$$(\mathbf{P} - \lambda^t \mathbf{S}) \mathbf{c}_k^t = \beta_k^t \mathbf{c}_k^t, \quad \text{for } k = 1, \dots, K$$

where  $\beta_1^t \leq \beta_2^t \leq \dots \leq \beta_K^t$  are the  $K$  smallest eigenvalues and  $\mathbf{c}_k^t$  is the eigenvector corresponding to the eigenvalue  $\beta_k^t$ , which constitutes the  $k$ th column of the  $L \times K$  matrix  $\mathbf{C}(\lambda^t)$ .

- (d) If  $\|\mathbf{C}(\lambda^t) - \mathbf{C}(\lambda^{t-1})\| \leq \sqrt{LK} \varepsilon$ , then break.
  - (3) Output  $\mathbf{C}^{\text{NC-ITR}} = \mathbf{C}(\lambda^t)$ .
- 

analysis. In other words, the solution is constrained to lie within the space spanned by the eigenvectors of  $\mathbf{S}$  corresponding to nonzero eigenvalues of  $\mathbf{S}$ . It is important to note that Algorithm 1 is globally and at least linearly convergent to the global minimum of the TR problem (Theorem 4.1 in [27]).

## 4.3. Discussion

After the secondary BS obtains the information of the spectral position of the primary system, it forms the matrices  $\mathbf{P}$  and  $\mathbf{S}$  and also the TR problem in (19). Then the TR problem can be solved by either of two methods GEVD and ITR. The calculation complexity of the NC-GEVD method is dominated by the calculation of inverse and EVD of two different  $L \times L$  matrices. The complexity order of each of them is  $O(L^3)$  [25]. At each iteration of the NC-ITR, there is the need for calculating the EVD of an  $L \times L$  matrix that dominates the other calculations. If the number of iterations for NC-ITR to be converged is assumed to be  $r$ , the computational complexity of NC-ITR is roughly  $r/2$  times greater than that of the NC-GEVD method. The BS should be designed resource-rich in terms of its computational

ability so that these calculations are feasible. Note that the complexity of both methods is independent of the spectral environment. The designed spreading codes are sent to the users by a signaling channel, and they are valid until the next spectral displacement of the PUs. This is the advantage of our sidelobe suppression method over the family of AIC-CC methods [14–16] and also AST method [17], because in these methods, the data of AIC tones and the AST data should be updated at every sent OFDM frame. The update of AIC (or CC) tones involves solving a least square problem. This requires calculation of SVD of a matrix whose size is dependent on the upsampling factor and the bandwidth occupied by the primary system [15].

When the spectral positions of the PUs change and the BS of the CR become aware of the changes, it must cease the transmission and adapt itself to the new environment like every overlay MC based CR. Thus, the BS designs the new codes and sends them to the SUs. If the spectral displacement of the PUs occurs frequently, the spreading code set must be updated frequently in order to deploy only the vacant subcarriers as well as suppressing the leaked sidelobe power to the spectral band of the PUs. In this way, the computational load of secondary BS for spreading code set design increases. Besides, the delay caused by the need for spreading code set update will disrupt the data transmission of the users frequently. In fact, these challenging issues are the intrinsic problems ahead of implementation of the CR networks. For example, the implementation of precoders for sidelobe suppression in MC systems [12,18–20], and the deployment of cooperative spectrum sensing approaches [28] encounter similar challenges in environments that change frequently. These challenges are the increase of the required computational ability and the time delay in the transmission. Therefore, the proposed spreading code sets are beneficial in the environments where the spectral displacement rate of the PUs is slow to moderate. For example, they are applicable for the situations similar to the IEEE 802.22 where the static allocation of the PUs' channels (TV channels) relaxes the timing requirements for the CR network.

It is important to note that because we have considered the synchronous downlink transmission, the optimal zero-lag cross-correlation constraint is sufficient for the designed code sets [29] that is fully satisfied by the  $\mathbf{C}^H \mathbf{C} = \mathbf{I}_K$  constraint.

## 5. SIMULATION RESULTS

The sidelobe suppression performances of the proposed non-contiguous MC-CDMA schemes, namely NC-GEVD and NC-ITR, are evaluated by using Monte Carlo computer simulations. A coherent downlink secondary communication system is considered that is allowed to transmit on unused parts of a fixed spectrum. The modulation scheme is 16-QAM, and the cyclic prefix length is  $\nu = 16$ . The averaged power spectra are procured from 5000 simulation runs. The upsampling factor is assumed to be  $N_s = 16$  in

order to provide good resolution for the spectrum analysis. Unless otherwise stated, the number of guard band tones is  $\gamma = 2$  in the simulations.

Two algorithms are used for performance comparison with the proposed schemes. The first is the conventional non-contiguous MC-CDMA in which the subcarriers located in the band of PUs and the guard band are turned off. Because the number of remaining data carriers can be any integer value, we need spreading codes that exist with arbitrary length. For this purpose, the complex orthogonal CI codes are deployed. When the orthogonal Hadamard–Walsh codes of the same length exist, it has been shown that the error performance of CI codes is the same as that of the Hadamard–Walsh codes [9,10]. We call this scheme as NC-CI. The second MC-CDMA scheme deploys AIC sidelobe suppression method by inserting AIC tones instead of guard band tones in the NC-CI, and so it is called NC-CI-AIC.

As the first scenario, assume that a primary transmitter is detected at the band covered by the subcarriers numbered from  $\#s_1 = 65$  to  $\#s_2 = 90$ . In this way, the number of data, PU-coincided and guard band subcarriers is  $(N_D, N_{PU}, N_{GB}) = (98, 26, 4)$ , and the fully loaded number of active users is  $K^{FL} = N_D = 98$ . The normalized power spectral density (PSD) of the proposed schemes is depicted in Figures 1 and 2 for  $K = 60$  and  $K = 82$  active users, respectively. The maximum value of the normalized PSD at the barred PU band is considered as the sidelobe suppression performance indicator of the different MC-CDMA schemes that is demonstrated by the horizontal line. From Figure 1, it is seen that the proposed NC-GEVD and NC-ITR schemes are able to fundamentally discard the leaked sidelobe power to the PU band. As mentioned in Section 4, the ITR algorithm is the optimal solution to the TR problem. So, the NC-ITR achieves  $-180$  dB sidelobe suppression that can be considered as zero leaked power. It also outperforms the NC-GEVD scheme because the GEVD is an approximation to the optimal solution of the TR problem. However, both

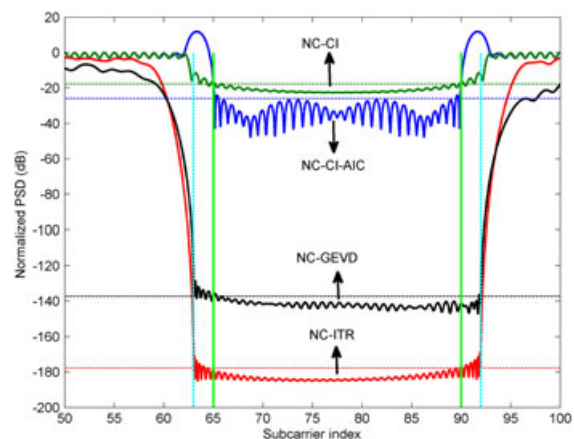


**Figure 1.** Normalized power spectral density for the first scenario when  $K = 60$ .

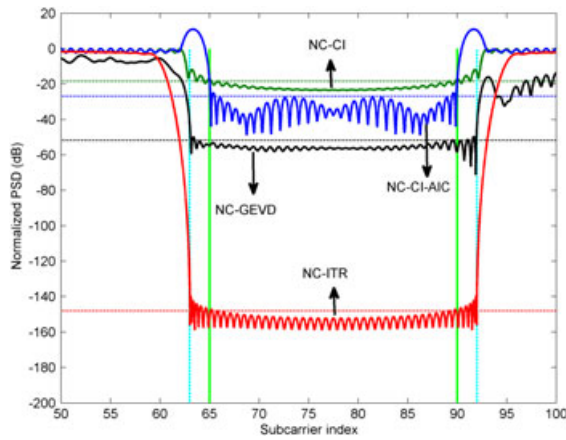


**Figure 2.** Normalized power spectral density for the first scenario when  $K = 82$ .

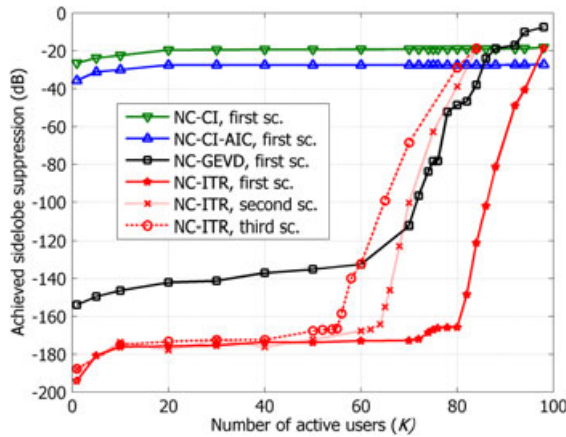


**Figure 3.** The achieved sidelobe suppression in decibels versus the number of active users for the three scenarios.

schemes outperform the NC-CI and NC-CI-AIC schemes that deploy subcarrier nulling and AIC methods for sidelobe suppression, respectively. Comparing Figures 1 and 2, it is observed that by increasing the number of users from  $K = 60$  to  $K = 82$ , the sidelobe suppression performance of NC-CI and NC-CI-AIC is unchanged, but the sidelobe suppression ability of the proposed schemes is decreased. This shows the dependency of their performance on the number of active users. To illustrate this, the maximum value of normalized PSD in the PU band versus the number of active users is depicted in Figure 3 for the four schemes. Two other scenarios are also considered for the comparison in this figure. Because the sidelobe suppression of the NC-CI and NC-CI-AIC are almost unchanged for different  $K$ , we can say that their sidelobe suppression performance is independent of  $K$ . For the proposed schemes, the NC-GEVD performance completely depends on  $K$  and is totally poor in comparison with the NC-ITR scheme. However, it considerably outperforms NC-CI-AIC for  $K \leq 86$ . When NC-ITR works at the fully loaded case

( $K = K^{\text{FL}} = N_{\text{D}}$ ), its performance is the same as the conventional NC-CI MC-CDMA scheme. But by slightly decreasing  $K$  to 80, the maximum leaked power of NC-ITR to the PU band decreases sharply to almost zero. So, the achieved sidelobe suppression can be controlled by the number of active users. Let us define  $K^0$  as the maximum number of active users that results in almost zero leaked power into the adjacent in-band primary transmission. On the basis of Figure 3, we have  $K^0 = 80$  for the first scenario. The value of  $K^0$  mainly depends on the spectral characteristics of the primary transmission. To show this, two scenarios are considered other than the first scenario. In the second scenario, the primary system occupies a larger bandwidth from subcarrier  $\#s_1 = 51$  to  $\#s_2 = 90$ , so  $(N_{\text{D}}, N_{\text{PU}}, N_{\text{GB}}) = (84, 40, 4)$ . In the third scenario, it is assumed that two spectrally disjoint PUs deploy parts of the secondary band coinciding with the subcarrier  $\#s_1 = 41$  to  $\#s_2 = 60$  and also from  $\#s_3 = 80$  to  $\#s_4 = 95$ , so we have  $(N_{\text{D}}, N_{\text{PU}}, N_{\text{GB}}) = (84, 36, 8)$ . Both the scenarios are considered in the way that the fully loaded number of users become the same, that is,  $K^{\text{FL}} = N_{\text{D}} = 84$ . In Figure 3, it can be seen that the behavior of NC-ITR is repeated for both new scenarios. When the system is fully loaded, NC-ITR acts as the deactivating subcarrier scheme (NC-CI), and by decreasing the number of active users, the sidelobe suppression performance of NC-ITR gradually becomes better. The graph of the first scenario falls off slightly sharper. However, comparing the second and third scenarios,  $K^0$  for two spectrally disjoint PUs (third scenario) is smaller than the one for a PU with the same bandwidth (i.e., the second scenario), although the values of  $K^{\text{FL}}$ ,  $N_{\text{D}}$  and  $N_{\text{PU}}$  are the same for them. So, when the bandwidth of the primary transmission is widened or it is non-contiguous, the amount of the decrement in  $K^0$  with respect to the fully loaded number of active users varies. For the third scenario, the normalized PSD of the proposed schemes are depicted in Figure 4 when  $K = 50$ . Because  $K \leq K^0$ , the NC-ITR is able to minimize the leaked power to both disjoint primary bands to zero. The NC-GEVD shows good performance of  $-130$  dB sidelobe suppression, while NC-CI-AIC only achieves  $-30$  dB suppression. Consequently, the proposed schemes, especially NC-ITR, are able to adapt themselves to any spectrum pattern deployed by the primary system depending on the number of active users. In order to further analyze this dependency for NC-ITR, we define  $d^0 = K^{\text{FL}} - K^0$  as the required decrement of  $K$  w.r.t.  $K^{\text{FL}}$  such that the leaked power to the adjacent primary band reaches zero. In Figure 5, for the 1-PU and 2-PUs cases (first and third scenarios, respectively), the value of  $d^0$  is plotted for different values of the data subcarriers, that is, different primary system's bandwidths. It is seen that the required decrement in  $K$ ,  $d^0$ , is larger when two PUs are present compared with the case where a single primary transmission uses the same bandwidth. For both scenarios, the change in  $d^0$  is not very large for different primary bandwidths (i.e., different  $N_{\text{D}}$  values). So,  $d^0$  (and hence  $K^0$ ) depends more on the spectral continuity of the primary transmission than the primary

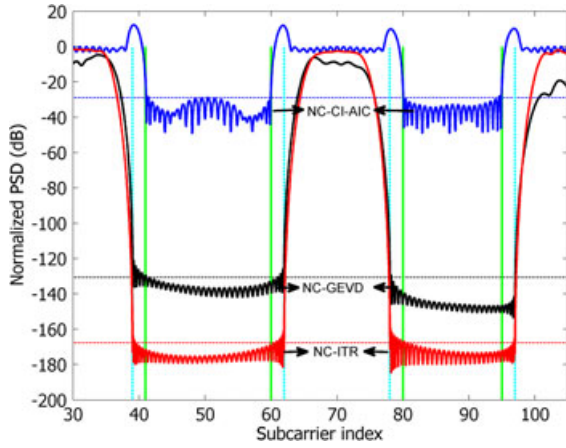


Figure 4. Normalized power spectral density for two narrow band spectrally disjoint primary users.

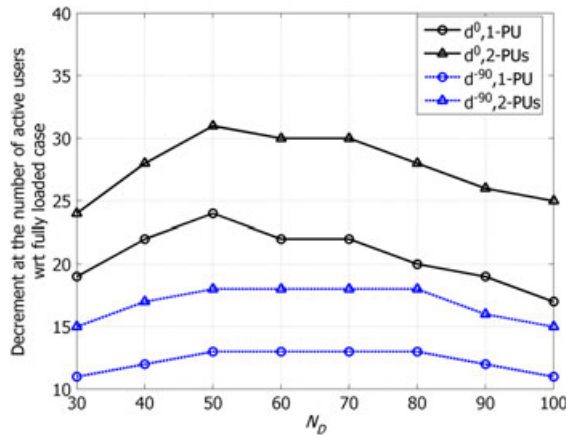


Figure 5. Comparison of the required decrement in the number of active users w.r.t. the fully loaded case needed for sidelobe power to be almost zero and for reaching  $-90$  dB.

bandwidth. Moreover, simulation results (not mentioned here for brevity) show that  $K^0$  also slightly depends on the spectral position of the primary transmission.

It is important to note that in practical applications, smaller sidelobe suppressions are sufficient. Considering sidelobe suppression of  $-90$  dB as [23], we define  $K^{-90}$  as the maximum number of active users such that when  $K \leq K^{-90}$ , the maximum leaked power to the PU band is below  $-90$  dB. It is clear that  $K^0 \leq K^{-90} \leq K^{FL}$ . Similar to  $d^0$ , the needed decrement in  $K$  with respect to  $K^{FL}$  to achieve below  $-90$  dB sidelobe suppression is expressed as  $d^{-90} = K^{FL} - K^{-90}$  and plotted in Figure 5 for both 1-PU and 2-PUs scenarios. Like  $d^0$ , for a given primary bandwidth,  $d^{-90}$  is larger when the primary transmission is not continuous (i.e., for 2-PUs scenario). Also, the variation of  $d^{-90}$  for different  $N_D$  values is small in both 1-PU and 2-PUs scenarios. Therefore, the secondary BS is able to control the amount of leaked power to the primary band

Table I. A set of spreading codes designed by iterative trace ratio when  $L = 16$  and  $K^{FL} = N_b = 13$ .

	$c_1$	$c_2$	$c_3$	$c_4$	$c_5$	$c_6$	$c_7$	$c_8$
$l = 0$	$-0.006 - 0.004i$	$-0.006 - 0.004i$	$0.004 + 0.003i$	$-0.109 - 0.0730i$	$0.09 + 0.06i$	$-0.453 - 0.302i$	$0.563 + 0.376i$	$0.130 + 0.0870i$
$l = 1$	$-0.002 - 0.006i$	$-0.003 - 0.007i$	$0.004 + 0.01i$	$0.0470 + 0.112i$	$0.0720 + 0.173i$	$-0.196 - 0.472i$	$-0.267 - 0.644i$	$-0.005 - 0.0130i$
$l = 2$	$-0.0250 + 0.102i$	$-0.0570 + 0.312i$	$0.0640 - 0.368i$	$0.107 - 0.538i$	$0.0840 - 0.424i$	$-0.0390 + 0.197i$	$0.0180 - 0.0890i$	$0.0280 - 0.141i$
$l = 3$	$-0.105 + 0.122i$	$0.473 - 0.499i$	$-0.291 + 0.303i$	$0.0290 - 0.0290i$	$0.144 - 0.144i$	$-0.143 + 0.143i$	$-0.0280 + 0.028i$	$0.185 - 0.185i$
$l = 4$	$0.456 - 0.103i$	$-0.474 + 0.117i$	$-0.4 + 0.0940i$	$-0.149 + 0.03i$	$-0.174 + 0.0350i$	$-0.181 + 0.0360i$	$-0.104 + 0.021i$	$0.315 - 0.0630i$
$l = 5$	$-0.229 - 0.09v$	$0.127 + 0.0420v$	$0.501 + 0.190i$	$-0.127 - 0.0520v$	$-0.485 - 0.201v$	$-0.123 - 0.0510i$	$-0.0980 - 0.041i$	$0.186 + 0.0770i$
$l = 6$	$0.0180 + 0.026i$	$-0.008 - 0.01i$	$-0.0690 - 0.097i$	$0.0320 + 0.048i$	$0.163 + 0.244i$	$0.096 + 0.143i$	$0.04 + 0.06i$	$-0.284 - 0.425i$
$l = 7$	$-0.0 - 0.001i$	$0.0 + 0.0i$	$0.0 + 0.005i$	$-0.0 - 0.004i$	$-0.0 - 0.0160i$	$0.0 - 0.01i$	$-0.0 - 0.005i$	$-0.0 + 0.0540i$
$l = 8$	$0.0 + 0.0i$	$0.0 + 0.0i$	$-0.001 + 0.001i$	$0.001 - 0.001i$	$-0.001 + 0.001i$	$-0.001 + 0.002i$	$0.0 + 0.0i$	$0.007 - 0.0110i$
$l = 9$	$0.0 + 0.0i$	$0.0 + 0.0i$	$-0.001 + 0.001i$	$0.002 - 0.001i$	$0.0 + 0.0i$	$-0.001 + 0.00i$	$0.001 + 0.0i$	$0.0130 - 0.005i$
$l = 10$	$0.0 + 0.0i$	$0.0 + 0.0i$	$-0.001 + 0.0i$	$0.002 + 0.0i$	$0.002 + 0.0i$	$0.001 + 0.0i$	$0.001 + 0.0i$	$0.0130 + 0.003i$
$l = 11$	$-0.001 - 0.001i$	$0.0 + 0.0i$	$-0.003 - 0.003i$	$0.004 + 0.004i$	$-0.01 - 0.01i$	$-0.009 - 0.009i$	$0.001 + 0.001i$	$-0.0380 - 0.038i$
$l = 12$	$0.01 + 0.0490i$	$0.004 + 0.0180i$	$0.02 + 0.0870i$	$-0.0210 - 0.105i$	$0.05 + 0.253i$	$0.0430 + 0.218i$	$-0.004 - 0.02i$	$0.1 + 0.502i$
$l = 13$	$0.134 - 0.326i$	$0.0550 - 0.133i$	$0.126 - 0.334i$	$-0.149 + 0.360i$	$0.168 - 0.407i$	$0.0970 - 0.233i$	$-0.0360 + 0.086i$	$0.0770 - 0.186i$
$l = 14$	$-0.550 + 0.369i$	$-0.269 + 0.179i$	$-0.224 + 0.161i$	$-0.0140 + 0.009i$	$0.0730 - 0.0490i$	$0.256 - 0.171i$	$-0.0430 + 0.028i$	$0.267 - 0.179i$
$l = 15$	$0.342 + 0.0i$	$0.212 + 0.0i$	$-0.0390 + 0.0i$	$0.676 + 0.0i$	$-0.250 + 0.0i$	$0.267 + 0.0i$	$0.0750 + 0.0i$	$0.263 + 0.0i$

by reducing the number of active users. The amount of reduction in  $K$  depends on the spectral characteristics of the primary transmission.

In order to gain some insight into the structure of the proposed codes, a set of spreading codes designed on the basis of the NC-ITR method is given in Table I. A different scenario (namely, fourth) is considered so that the results are presentable. The number of subcarriers and the length of CP are considered to be  $L = 16$  and  $\nu = 2$ , respectively. One PU uses the part of spectrum covering the subcarriers numbered 8, 9 and 10. Besides, no guard band subcarriers are inserted. So, we have  $(N_D, N_{PU}, N_{GB}) = (13, 3, 0)$ . The fully loaded number of active users is  $K^{FL} = N_D = 13$ . Simulations (not depicted here) show that when the number of active users is set to  $K = 8$ , the achieved sidelobe suppression is  $-100$  dB. So, the set of eight spreading codes is presented in Table I with the values rounded up to three decimal points. The proposed methods try to design the codes such that the part of available power leaked to the band of primary transmission is minimized with respect to the allocated power to the secondary transmission. The complex values of the code chips are calculated on the basis of this goal, and they do not follow any obvious pattern except that the chips located at the PU band are forced to nearly zero.

It is important to note that for all the scenarios considered, the iterative NC-ITR algorithm converges after at most 10 iterations (the convergence plots are not given for the sake of brevity). So, referring to the complexity discussion in Section 4, it is revealed that complexity of the optimal NC-ITR method is slightly greater than the approximate NC-GEVD method. Consequently, if the BS is not limited by its computational resources and its timing requirements, the NC-ITR is the best solution regarding its sidelobe suppression ability.

The BER performances of the schemes are compared in Figure 6 versus signal-to-noise ratio for the PU transmission scenario of Figure 1. To have a fair comparison, the allocated power to the MC-CDMA symbol in the

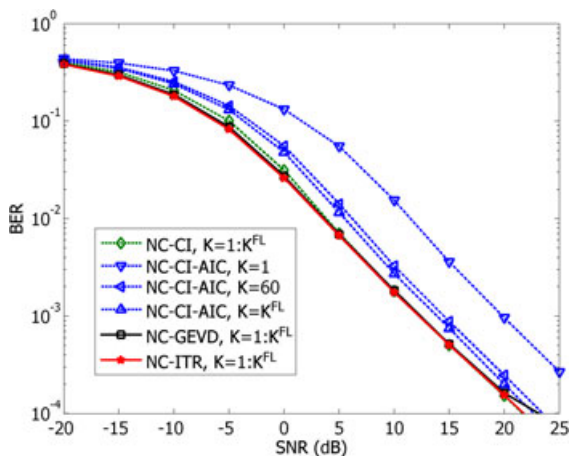


**Figure 6.** Bit error rate versus signal-to-noise ratio for the first scenario.

four schemes is the same. The frequency selective channel between the BS and each user has been realized on the basis of an exponential power delay profile with  $L_c = 16$  resolvable paths where the exponential decay factor is assumed to be  $\beta = 0.1$ . It can be seen that like NC-CI, the NC-ITR and NC-GEVD are able to completely eliminate multiuser interference even in the fully loaded case where  $K^{FL} = 98$ , because the orthogonality of the spreading codes is preserved in synchronous downlink transmission and each receiver is able to completely reject multiuser interference. However, NC-CI-AIC suffers from BER performance loss with respect to the other schemes, because the amount of power spent on the AIC tones is not available for data transmission. It is also seen that by increasing  $K$ , the BER performance is improved because the AIC tones are designed on the basis of the sum of the users' data. While  $K$  is increased, the ratio of power spent on the AIC tones to the power consumed for the transmission of the data of the desired user is decreased. So, the signal-to-noise ratio for each of the users is improved, which results in better BER performance while  $K$  is increased.

## 6. CONCLUSIONS

In this paper, two novel complex spreading code sets are proposed for non-contiguous MC-CDMA based CR network with the goal of suppressing spectral sidelobes at the spectral band used by the PUs. Doing so, the need for extra processing for sidelobe suppression is resolved. The code sets are designed as solutions to a TR optimization problem, called NC-GEVD and NC-ITR. The NC-ITR outperforms the NC-GEVD because it is the optimal solution to the TR problem. The achieved sidelobe suppression level by both schemes is remarkable and depends on the number of active users. Simulation results show that by accepting a slight decrease in the number of active users with respect to the fully loaded case, any level of sidelobe suppression is achievable. It is shown that the required amount of decrement is a function of spectral characteristics of the primary transmission. In addition, because the codes are designed to be orthogonal, they do not degrade bit error performance.

## ACKNOWLEDGEMENT

This work was supported in part by Iranian Research Institute for ICT (ICT).

## REFERENCES

1. Mitola J. Cognitive radio for flexible mobile multimedia Communications, In *Proceedings of International Workshop on Mobile Multimedia Communications*, San Diego, CA, USA, November 1999; 3–10.
2. Attar A, Nakhai MR, Aghvami AH. Cognitive radio transmission based on direct sequence MC-CDMA.

- IEEE Transactions on Wireless Communication* 2008; **7**(4): 1157–1162.
3. Chakravarthy V, Li X, Wu Z, Temple MA, Garber F, Kannan R, Vasilakos A. Novel overlay/underlay cognitive radio waveforms using SD-SMSE framework to enhance spectrum efficiency—part I: theoretical framework and analysis in AWGN channel. *IEEE Transactions on Communications* 2009; **57**(12): 3794–3804.
  4. Chakravarthy V, Li X, Zhou R, Wu Z, Temple M. Novel overlay/underlay cognitive radio waveforms using SD-SMSE framework to enhance spectrum efficiency—part II: analysis in fading channels. *IEEE Transactions on Communications* 2010; **58**(6): 1868–1876.
  5. Sarath D, Nolan KE, Sutton PD, Doyle LE. Exploring the reconfigurability options of multi-carrier CDMA in cognitive radio systems, In *Proceedings of IEEE International Symposium on Personal Indoor and Mobile Radio Communications*, Athens, Greece, September 2007; 1–5.
  6. Weiss T, Jondral F. Spectrum pooling: an innovative strategy for the enhancement of spectrum efficiency. *IEEE Communications Magazine* 2004; **42**(3): S8–S14.
  7. Mahmoud H, Yucek H, Arslan H. OFDM for cognitive radio: merits and challenges. *IEEE Wireless Communications Magazine* 2009; **16**(2): 6–15.
  8. Azarnasab E, Kempter N, Patwari N, Farhang-Boroujeny B. Filterbank multicarrier and multicarrier CDMA for cognitive radio systems, In *Proceedings of IEEE CrownCom*, Orlando, FL, USA, August 2007; 472–481.
  9. Wu Z, Ratazzi P, Chakravarthy VD, Hong L. Performance evaluation of adaptive non-contiguous MC-CDMA and non-contiguous CI/MC-CDMA for dynamic spectrum access, In *Proceedings of IEEE CrownCom*, Singapore, May 2008; 1–6.
  10. Rajabzadeh M, Khoshbin H. Receiver design for downlink MIMO MC-CDMA in cognitive radio systems, In *Proceedings of IEEE International Symposium on Personal Indoor and Mobile Radio Communications*, Istanbul, Turkey, September 2010; 785–789.
  11. Li X, Chakravarthy VD, Wang B, Wu Z. Spreading code design of adaptive non-contiguous SOFDM for dynamic spectrum access. *IEEE Journal on Selected Topics in Signal Processing* 2011; **5**(1): 190–196.
  12. Chung CD. Spectrally precoding for rectangularly pulsed OFDM. *IEEE Transactions on Communications* 2008; **56**(9): 1498–1510.
  13. Weiss T, Hillenbrand J, Krohn A, Jondral FK. Mutual interference in OFDM-based spectrum pooling systems, In *Proceedings of IEEE Vehicular Technology Conference*, Milan, Italy, May 2004; 1873–1877.
  14. Qu D, Wang Z, Jiang T. Extended active interference cancellation for sidelobe suppression in cognitive radio OFDM systems with cyclic prefix. *IEEE Transactions on Vehicular Technology* 2010; **59**(4): 1689–1695.
  15. Huang S, Hwang C. Improvement of active interference cancellation: avoidance technique for OFDM cognitive radio. *IEEE Transactions on Wireless Communications* 2009; **8**(12): 5928–5937.
  16. Brandes S, Cosovic I, Schnell M. Reduction of out-of-band radiation in OFDM systems by insertion of cancellation carriers. *IEEE Communications Letters* 2006; **10**(6): 420–422.
  17. Mahmoud HA, Arslan H. Sidelobe suppression in OFDM based spectrum sharing systems using adaptive symbol transition. *IEEE Communications Letters* 2008; **12**(2): 133–135.
  18. Xu R, Chen M. A precoding scheme for DFT-based OFDM to suppress sidelobes. *IEEE Communications Letters* 2009; **13**(10): 776–778.
  19. Beek JVD. Sculpting the multicarrier spectrum: a novel projection precoder. *IEEE Communications Letters* 2009; **13**(12): 881–883.
  20. Beek JVD, Berggren F. N-continuous OFDM. *IEEE Communications Letters* 2009; **13**(1): 1–3.
  21. Cosovic I, Brandes S, Schnell M. Subcarrier weighting: a method for sidelobe suppression in OFDM systems. *IEEE Communications Letter* 2006; **10**(6): 444–446.
  22. Cosovic I, Mazzoni T. Sidelobe suppression in OFDM spectrum sharing systems via additive signal method, In *Proceedings of IEEE Vehicular Technology Conference*, Dublin, Ireland, April 2007; 2692–2696.
  23. Yuan Z, Wyglinski AM. On sidelobe suppression for multicarrier-based transmission in dynamic spectrum access networks. *IEEE Transactions on Vehicular Technology* 2010; **59**(4): 1998–2006.
  24. Jia Y, Nie F, Zhang C. Trace ratio problem revisited. *IEEE Transactions on Neural networks* 2009; **20**(4): 729–735.
  25. Golub GH, Loan CFV. *Matrix Computations*. Johns Hopkins University Press: Baltimore (MD), USA, 1996.
  26. Wang H, Yan S, Xu D, Tang X, Huang T. Trace ratio vs. ratio trace for dimensionality reduction, In *Proceedings of IEEE Computer Vision and Pattern Recognition*, Minneapolis, MN, USA, June 2007; 1–6.
  27. Zhang L, Liao L, Ng MK. Fast algorithms for the generalized Foley–Sammon discriminant analysis. *SIAM Journal on Matrix Analysis and Applications* 2010; **31**(4): 1584–1605.

28. Yucek T, Arslan H. A survey of spectrum sensing algorithms for cognitive radio applications. *IEEE Communications Surveys & Tutorials* 2009; **11**(1): 116–130.
29. Hara S, Prasad R. Overview of multicarrier CDMA. *IEEE Communications Magazine* 1997; **35**(12): 126–133.

## AUTHORS' BIOGRAPHIES



**Morteza Rajabzadeh** received his BSc and MSc degrees (both with honors) in electrical engineering in 2005 and 2008, respectively, from Ferdowsi University, Mashhad, Iran. At present, he is a PhD candidate at the Department of Electrical and Computer Engineering, Ferdowsi



**Hossein Khoshbin** received his BSc degree in electronics engineering and his MSc degree in communications engineering in 1985 and 1987, respectively, both from Isfahan University of Technology, Isfahan, Iran. He received his PhD degree in communications engineering from the University of Bath, UK, in

2000. He is currently an assistant professor at the Department of Electrical and Computer Engineering, Ferdowsi University, Mashhad, Iran. His research interests include communication theory and digital and wireless communications.